

# The vanishing limit of the square-well fluid: the adhesive hard sphere model as a reference system

J. Largo<sup>1,2\*</sup>, M. A. Miller<sup>3</sup>, F. Sciortino<sup>1,2</sup>

<sup>1</sup>*Dipartimento di Fisica, <sup>2</sup>INFM-CRS-SOFT, Università di Roma La Sapienza, Piazzale A. Moro 2, 00185 Roma, Italy and <sup>3</sup> University Chemical Laboratory, Lensfield Road, Cambridge CB2 1EW, United Kingdom and <sup>1</sup>largojulio@gmail.com, <sup>3</sup>mam1000@cam.ac.uk, <sup>2</sup>francesco.sciortino@phys.uniroma1.it*

## Abstract

We report a simulation study of the gas-liquid critical point for the square-well potential, for values of well width  $\delta$  as small as 0.005 times the particle diameter  $\sigma$ . For small  $\delta$ , the reduced second virial coefficient at the critical point  $B_2^{*c}$  is found to depend linearly on  $\delta$ . The observed weak linear dependence is not sufficient to produce any significant observable effect if the critical temperature  $T_c$  is estimated via a constant  $B_2^{*c}$  assumption, due to the highly non linear transformation between  $B_2^{*c}$  and  $T_c$ . This explains the previously observed validity of the law of corresponding states. The critical density  $\rho_c$  is also found to be constant when measured in units of the cubed average distance between two bonded particles  $(1 + 0.5\delta)\sigma$ . The possibility of describing the  $\delta \rightarrow 0$  dependence with precise functional forms provides improved accurate estimates of the critical parameters of the adhesive hard-sphere AHS model.

PACS numbers: 05.20.Jj, 61.20.Ja, 64.70.Ja

---

\* Corresponding author. Present address: Dpt. de Física Aplicada, Universidad de Cantabria, Avd. Los Castros s/n Santander 39004, Spain.

## I. INTRODUCTION

Investigation of protein and colloidal systems has focused the attention of the scientific community on the phase-diagram behavior of short-range attractive potentials and of the role of the range of interaction in controlling the thermodynamic and dynamic properties of the system[1, 2, 3, 4, 5]. Colloidal particles, due to their nano or microscopic size are often characterized by effective interactions[6] whose range is significantly smaller than the particle diameter. Under these conditions, it has been argued that the actual shape of the potential is irrelevant and that the thermodynamics[7], as well as the dynamics[8], of different systems approximately satisfy an extended law of corresponding states[9]. This law allows for a comparison between different systems, once the effective diameter of the particle is known (i.e., when the repulsive part of the interaction can be mapped into an equivalent hard-sphere diameter [10]). It has been proposed that the second virial coefficient, normalized by the corresponding hard-sphere second virial coefficient,  $B_2^*$  may act as a proper scaling variable. Therefore systems with equal second virial coefficient and effective diameter should have similar thermodynamical properties.

The adhesive hard-sphere (AHS) potential[11], the limiting behavior of an infinitesimal interaction range coupled to infinite interaction strength such that  $B_2$  is finite, has also received significant attention. For this potential  $B_2^* = 1 - 1/4\tau$ , where  $\tau$ , which acts as an effective scaled temperature, is the so-called stickiness parameter. Despite the known thermodynamic anomalies[12], an analytic evaluation of the (metastable) critical point within the Percus-Yevick closure with both the energy and the compressibility routes for this potential is available[11, 13]. In the energy route the critical point is located at  $B_2^{*c} = -1.1097$  ( $\tau_c = 0.1185$ ) and number density  $\rho = 0.609$ .

The availability of analytic predictions for this model has favored its application in the interpretation of experimental data for several disparate colloid (and protein) systems[2, 3, 4, 5, 14, 15, 16], an application whose validity has been reinforced by the extended law of corresponding states. For this reason, it is important to try to accurately estimate the properties of the AHS model as a reference, to support existing predictions or to suggest improvements to available theoretical approaches. Numerical simulations of the AHS model have been attempted in the past[17, 18, 19]. A recent effort in the direction of evaluating the phase diagram of the model has been provided by Miller and Frenkel[20], based on an

ingenious identification of the appropriate Monte Carlo (MC) moves for this potential[17, 18]. Their study provides an estimate of the location of the critical point at  $B_2^{*c} = -1.21(1)$  ( $\tau_c = 0.1133(5)$ ) and  $\rho_c = 0.508(10)$ .

In this article we propose a different approach to the numerical evaluation of the critical properties of the AHS model, based on extrapolation of standard grand canonical MC simulation results for a sequence of square well (SW) potentials with progressively smaller attraction ranges  $\delta$  (down to  $\delta = 0.005$ , in units of the hard-sphere diameter  $\sigma$ ).

The SW potential is defined as:

$$U(r) = \begin{cases} \infty & \text{if } r \leq \sigma \\ -\epsilon & \text{if } \sigma < r \leq \sigma + \delta\sigma \\ 0 & \text{if } r > \sigma + \delta\sigma \end{cases} \quad (1)$$

The SW fluid has been profusely studied [21, 22, 23, 24, 25, 26, 27] for  $\delta > 0.1$ . It has been shown[24, 25] that for  $\delta \lesssim 0.25$  gas-liquid separation becomes metastable with respect to the fluid-solid equilibrium. Despite its metastable character, investigation of smaller  $\delta$  values retains its importance, since the crystallization time is often much longer than the experimental one and gas-liquid phase separation is readily accessed (an effect facilitated by the large difference between the fluid density and the crystal density and, in experiments, by the intrinsic sample polydispersity) .

Despite the importance of the SW model in relation to the AHS potential, no studies of the  $\delta$ -dependence of the critical point location has been previously reported for very small  $\delta$ . This is in large part due to the fact that for smaller and smaller  $\delta$ , the critical temperature significantly decreases. Indeed, according to the constant  $B_2^{*c}$  prediction of Noro and Frenkel[7], it should vary as

$$\frac{k_B T_c}{\epsilon} = \left[ \ln \left( 1 + \frac{1 - B_2^{*c}}{(1 + \delta)^3 - 1} \right) \right]^{-1} \quad (2)$$

making bond-breaking (changes of the particle energy of order  $\epsilon$ ) events rarer and rarer in the simulation. Moreover, the size of the translational step in the MC code is of the order of  $\delta$ . On the other hand, the location of the critical point becomes more and more metastable which, in principle, poses a limit to the smallest  $\delta$  which can be studied.

Despite these numerical difficulties, we have been able to estimate the location of the critical point down to  $\delta = 0.005\sigma$ . We present here the  $\delta$  dependence of the critical temperature and density and the values of the second virial coefficient and energy at the critical

point. In all cases, a short linear extrapolation to  $\delta = 0$  provides novel accurate estimates of the corresponding quantities for the AHS model.

## II. MONTE CARLO SIMULATIONS

We have simulated the SW system in the grand canonical (GC) ensemble in order to locate the gas-liquid critical point for different  $\delta$  values. The critical point is identified by mapping the grand canonical density distribution onto the universal Ising model distribution, following the method described by Bruce and Wilding[28]. Histogram reweighting [29] was used to achieve an accurate estimate of the critical point, and the field mixing parameter was always found to be negligible. We define a Monte Carlo step as one hundred trial moves, with an average of 95% translation and 5% trial insertions or removals of one particle in the system. A translational move is defined as a displacement in a random direction by a random amount between  $\pm\delta/2$ . We simulate different realizations of the same system (at the same chemical potential and temperature) to improve statistics. Simulations lasted more than  $10^7$  MC steps. We have studied cubic boxes of side  $5\sigma$  and/or  $8\sigma$ , to estimate the importance of finite-size effects. Additionally, for  $\delta = 0.05$  we have studied several other box sizes to estimate the deviation of the value of the critical parameter for the bulk limit case. Proper finite size studies for  $\delta < 0.05$  are at this moment numerically prohibitive. Histogram reweighting was used to map the density distribution of the fluid onto the universal critical order parameter distribution of the Ising model[29], thereby reaching an accurate estimate of the critical point. The field mixing parameter was always been found to be negligible.

We have occasionally observed a transition to a more dense stable phase, signaling that indeed the values of the chemical potential studied admit metastable fluid solutions. In all cases where a transition to a more dense phase was observed, the simulation was interrupted and the 10% of configurations saved just before the transition were disregarded. This procedure is shown graphically in Fig.-1.

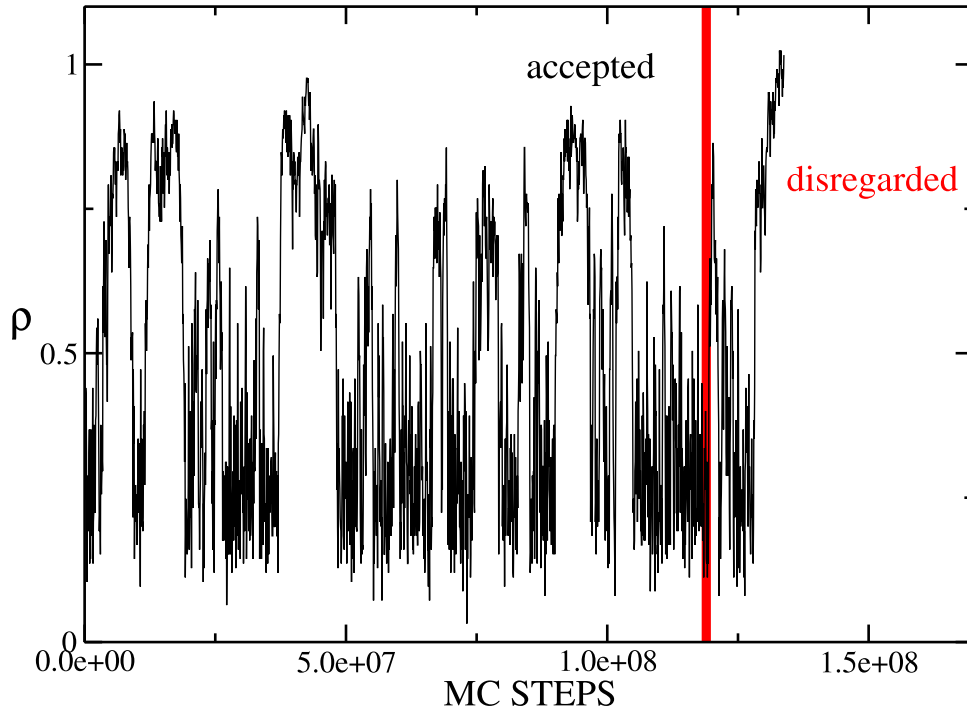


FIG. 1: Density evolution for a single run of a SW fluid with  $\delta=0.01$ ,  $T^* = 0.233$ , and  $\mu/kT = -2.41$  (close to the critical point). At long time, a transition to a dense phase is observed and, consequently the simulation on the right side of the vertical line is disregarded.

### III. RESULTS

Fig.-2-(a) and (b) show the  $\delta$  dependence of the critical temperature and the corresponding critical second virial coefficient  $B_2^{*c}$ . For SW, the virial can be calculated as

$$B_2^*(T) = 1 - ((\delta + 1)^3 - 1)(e^{1/T} - 1) \quad (3)$$

For small  $\delta$ , a clear linear dependence of  $B_2^{*c}$  is observed. The data are well represented by a functional form  $B_2^{*c}(\delta) = -1.174 - 1.774 \delta$ . The extrapolated value of  $B_2^{*c}$  for  $\delta = 0$  ( $B_2^{*c} = -1.174$ ) is slightly higher than the value  $-1.21(1)$  estimated by Miller and Frenkel for the AHS potential. The  $\delta$  dependence of  $B_2^{*c}$  formally violates the idea that  $B_2^{*c}$  is the correct scaling variable for collapsing the phase-diagram of different short-range attractive potentials

onto a single master curve. Nevertheless, the constant  $B_2^{*c}$  approximation is sufficiently good to explain the  $T_c$  dependence, due to the non-linearity of the transformation (Eq. 2). To prove this point we show in Fig.-2-(a)  $T_c$  predicted according to  $B_2^{*c} = -1.174$ . In this representation, the assumption of constant  $B_2^{*c}$  is sufficient to describe the  $\delta$  dependence of  $T_c$  up to  $\delta = 0.05$ , with an error less than 1% (growing with  $\delta$ ).

Next we compare the energy per particle of the system at the critical point in Fig.-2-(c), to provide a measure of the number of contacts per particle. This quantity also shows a linear dependence on  $\delta$ .

The study of the  $\delta$  dependence of the critical density  $\rho_c$  has received considerably less attention than the  $\delta$  dependence of  $T_c$ . Recently Ref.[30] suggested a plausible relation for the  $\delta$  dependence of  $\rho_c$  in the limit of small well width:

$$\rho_c(\delta) = \frac{\rho_c(0)}{(1 + \delta/2)^3}, \quad (4)$$

The relation is based on the hypothesis that  $\rho_c$  should be constant if measured using the average distance between two bonded particles  $(1 + \delta/2)\sigma$  as the unit of length. The relation was also supported by a potential energy landscape interpretation of the generalized law of corresponding states[31] which shows that configurations with the same Boltzmann weight are generated under an isotropic scaling (to change the inter-particle distances preserving the same bonding pattern) and a simultaneous change of both  $\delta$  and  $T$  such that the bond free-energy remains constant.

Figure 3-(a) shows the calculated evolution of the critical density with the range of the interaction. It also reports previous estimates for the same system[4] as well as the critical density for the AHS model from Ref.[20]. As the range of the SW potential is reduced, the critical density becomes higher, since a higher local density is required to generate bonded configurations. Data for  $\delta < 0.1\sigma$  are properly represented by Eq. 4, with a resulting fitting parameter  $\rho(0) = 0.552$ . This value is significantly higher than the AHS critical density  $\rho_c = 0.508$  reported in Ref.-[20].

For completeness we show in Figure 3-(b) the  $\delta$  dependence of  $\mu_c/k_B T_c$ , where  $\mu_c$  is the value of the chemical potential at the critical point.  $\mu_c/k_B T_c$  also shows a linear dependence, with an intercept at  $-2.394$ , corresponding to a critical activity  $\exp(\mu_c/k_B T_c) = 0.091$ , to be compared with the corresponding value of 0.087 of Miller and Frenkel.

It is known that the finite size of the system modifies the position of the critical point [32].

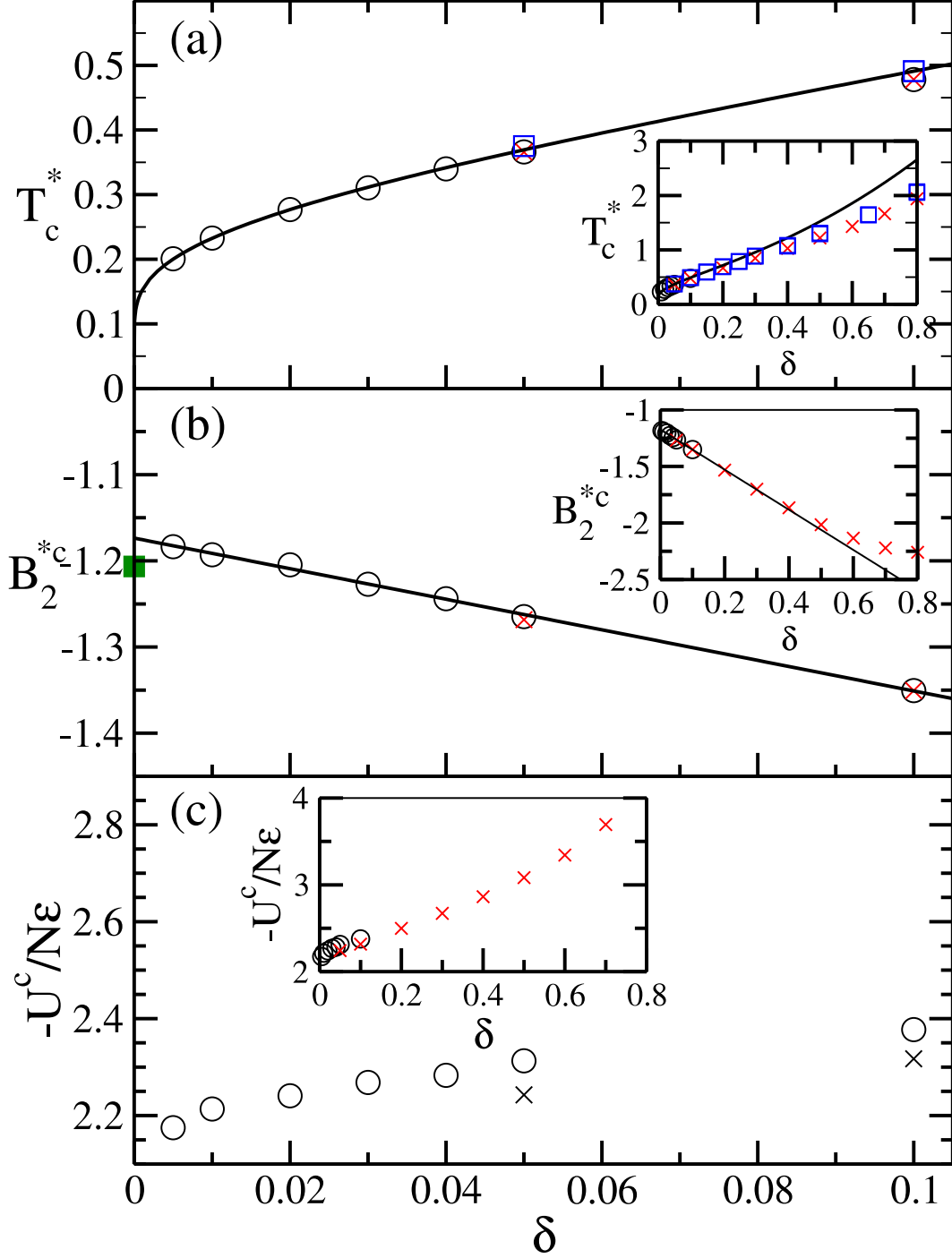


FIG. 2: Dependence of the critical temperature (a), of the second virial coefficient (b) and of the potential energy (c) on the range of the potential  $\delta$ . Circles and crosses label simulation data of this work with box sides  $5\sigma$  and  $8\sigma$  respectively. The line in (a) is the theoretical prediction for the critical temperature provided by Eq.2. The line in (b) corresponds to the best linear fit of the simulation data for  $\delta \leq 0.10$  ( $-1.174 - 1.774\delta$ ). Open squares correspond to the simulation data from Ref. [4]. Filled squares are the AHS  $B_2^{*c}$  result from Ref. [20]. The inset presents the whole range of  $\delta$  values studied.

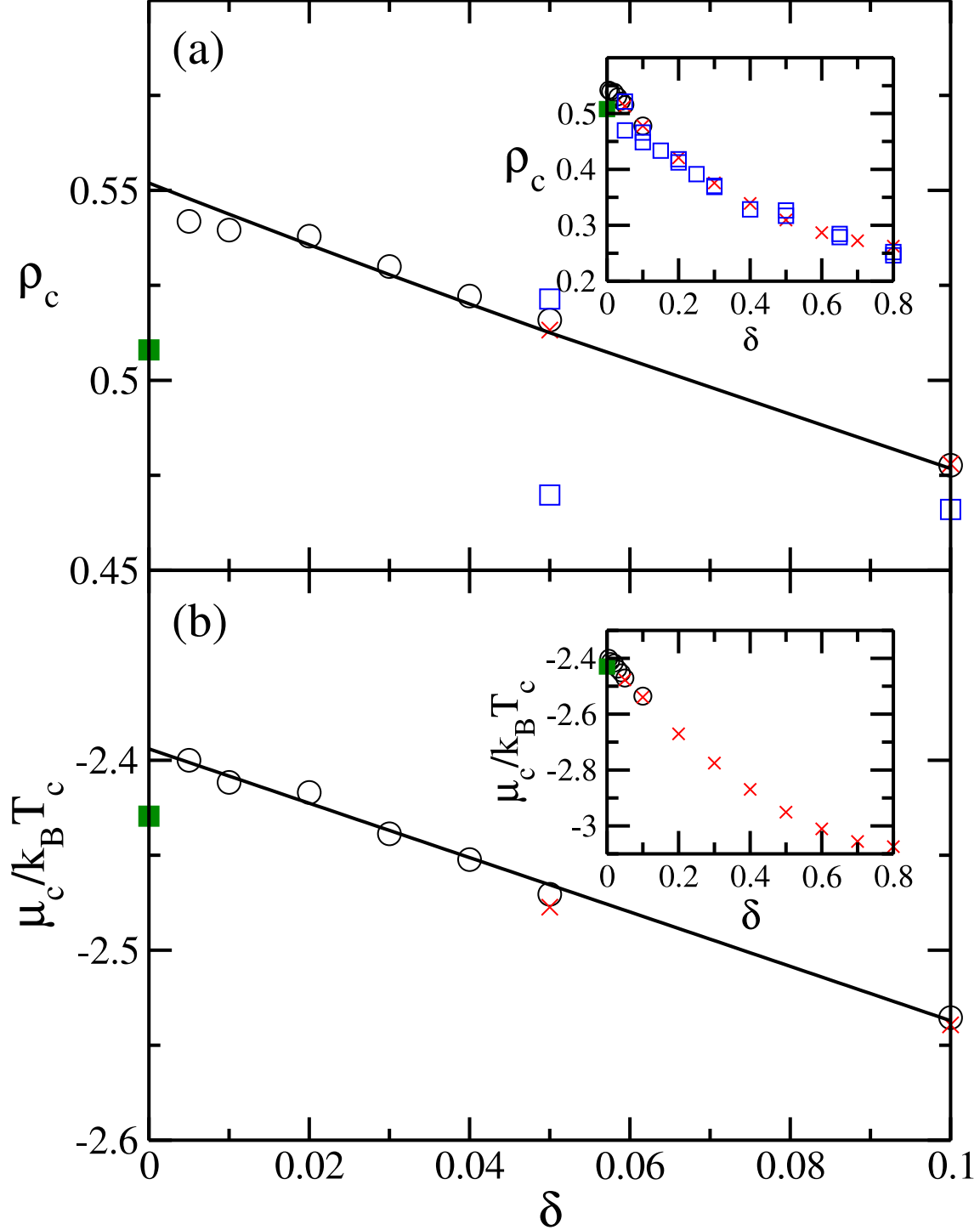


FIG. 3: Evolution of the critical density (a), and chemical potential (b) with the range of the potential  $\delta$ . Circles and crosses correspond to box sides  $L = 5\sigma$  and  $L = 8\sigma$  respectively. Empty squares in (a) are data from Ref. [4]. The lines correspond to the best fit of (a)  $\rho_c$  for  $\delta \leq 0.10$  ( $0.5519/(1 + \delta/2)^3$ ) and (b)  $\mu_c/k_B T_c$  for  $\delta \leq 0.10$  ( $-2.394 - 1.431\delta$ ). Filled squares represent AHS results from Ref. [20]. The inset presents the whole range of  $\delta$  values studied in this work.



A precise estimate of the critical point requires a complete finite-size scaling study to extrapolate the results to an infinite system. We have not attempted to perform such a careful study since it would be computationally prohibitive for the small ranges studied here and we have limited ourselves to four different box sizes ( $L = 5, 6, 8$  and  $10$ ) for  $\delta = 0.05$  only. The results are reported in table I. As already suggested by the minor differences in the  $L = 5$  and  $L = 8$  data shown in the previous figures, no significant changes in the critical parameters are observed. From the scatter in the data (similar to that found by Miller and Frenkel[20]) it is possible to estimate errors in the critical parameters. The resulting values of and errors in the critical parameters are  $T_c = 0.3658 \pm 0.0005$ ,  $\rho_c = 0.513 \pm 0.008$  and  $\mu_c = 0.9064 \pm 0.0008$ . These values of the critical temperature and density suggest that the Percus-Yevick energy route [13] is even better than previously thought, despite the fact that the compressibility route [11] results seem to be more often used and cited.

TABLE I: Critical parameters for the SW system of  $\delta = 0.05$  obtained with four different boxes of side  $L = 5, 6, 8, 10$ .

| $L$ | $T_c$  | $\rho_c$ | $\mu_c$ |
|-----|--------|----------|---------|
| 5   | 0.3660 | 0.516    | -0.9042 |
| 6   | 0.3660 | 0.516    | -0.9051 |
| 8   | 0.3658 | 0.513    | -0.9062 |
| 10  | 0.3657 | 0.511    | -0.9069 |

#### IV. DISCUSSION

Our study provides a set of values for the limiting AHS case, based on an accurate extrapolation of the critical parameters of the SW potential to  $\delta \rightarrow 0$ . These values are outside the error bars of Miller and Frenkel's investigation. In particular, both the critical density and the critical virial appear to be higher than the previous estimates.

The special techniques employed in the simulation of the AHS system [18, 20, 33] only consider moves that make or break up to three contacts. A particle can readily gain more than three contacts, since higher coordination states are established by a succession of such moves. Apparently, however, the constraint on the possible moves disfavors the formation

of small nuclei of solid phases, since crystallization was extremely rarely observed with this algorithm, and then only in fluids with a very high mean reduced density (greater than 0.9). In the SW simulation, the transient solid-like nuclei are more readily formed (and indeed we do occasionally observe crystallization during the simulation) suggesting that the SW simulations sample a larger region of configuration space than that accessible with the AHS algorithm. This could indeed explain why the critical density extrapolated from the SW simulations is significantly higher than that calculated previously.

To support this interpretation we have compared the distribution of the number of contacts per particle (proportional to the energy of the particle) for the AHS and a SW with  $\delta = 0.01$  at the same virial coefficient (slightly above the critical one) and same density for three different state points. The results of MC simulations in the NVT canonical ensemble, for different densities are reported in Fig. 4. The distributions of the number of contacts per particle are coincident for low densities, but discrepancies appear as the density is increased, confirming that the algorithm used in Ref. [20] explores configurations with a somewhat smaller coordination number than does the standard MC SW simulation. Figure 4 nevertheless confirms that the AHS algorithm permits the formation of high coordination states. To avoid any potential artifact due to the *a priori* unknown mapping in the density between the AHS and the SW potential, we have also repeated the calculation at a lower density, scaled according to Eq. 4. However, as shown in Fig. 4, even when the density is scaled to account for the different bond distance in the AHS and SW models, at high density the disagreement between the two set of simulations remains.

## V. CONCLUSIONS

We have reported a simulation study aimed at evaluating the dependence of the critical parameters of the short-range square well potential for interaction ranges approaching zero, down to  $\delta = 0.005\sigma$ . The resulting values for  $B_2^{*c}$  and  $\beta_c\mu_c$  in the range  $0.005 < \delta < 0.1$  are very well described by a linear dependence on  $\delta$ , providing an estimate for the  $\delta \rightarrow 0$  limit. From the resulting value of  $B_2^{*c}$  at  $\delta = 0$ , it is possible to evaluate also the corresponding critical value of the AHS model via the relation  $B_2^* = 1 - 1/4\tau$ . In the same range, the critical density is well represented by the previously proposed functional form of Eq. 4. More

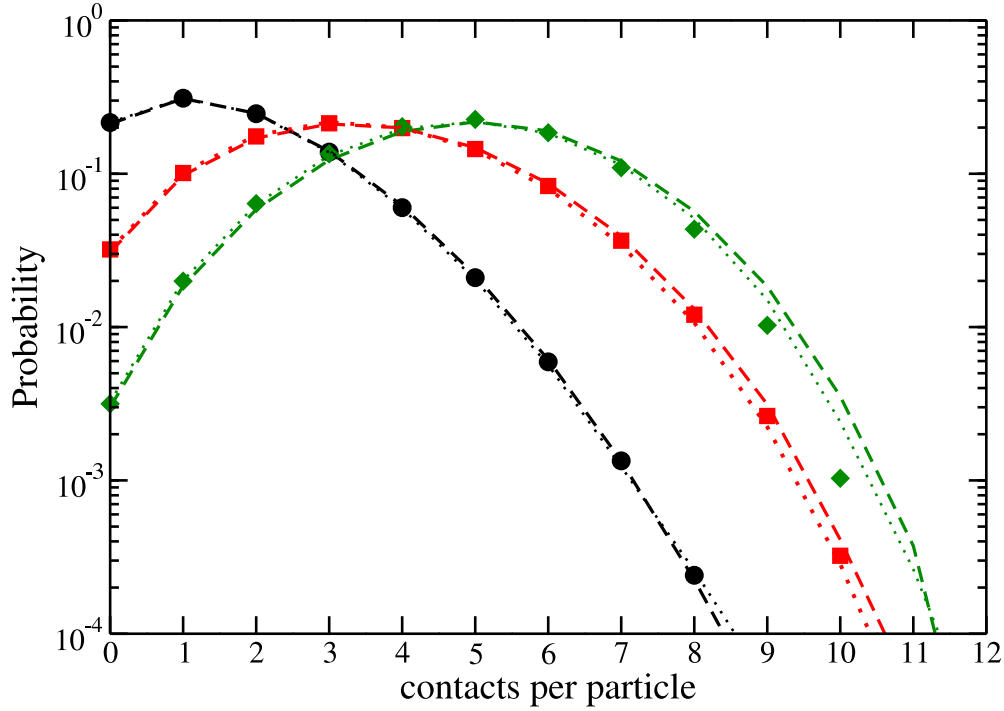


FIG. 4: Probability distribution of the number of contacts per particle for the AHS system and the SW with  $\delta = 0.01$ , for different densities. The comparison has been made at a slightly supercritical stickiness parameter  $\tau=0.120$ , in the case of the AHS, and the corresponding temperature provided by Eq. 2 for the SW of  $\delta = 0.01$ . The simulations were performed in the NVT canonical ensemble with volume  $V = 512\sigma^3$ . Symbols correspond to AHS simulation data, for  $\rho=0.195$  (circles), 0.488 (squares), 0.781 (diamonds). Dashed lines correspond to SW simulation data and dotted lines to SW simulations at the rescaled densities (see Eq. 4) 0.192, 0.481, 0.770, respectively.

precisely, our extrapolation for the AHS limit is:

$$B_2^{*c}(\delta = 0) = -1.174 \pm 0.002 \quad (5)$$

$$\tau_c = 0.1150 \pm 0.0001 \quad (6)$$

$$\rho_c(\delta = 0) = 0.552 \pm 0.001 \quad (7)$$

$$\beta_c \mu_c(\delta = 0) = -2.394 \pm 0.001 \quad (8)$$

TABLE II: Critical point parameters for the SW fluid for width  $\delta$ , resulting from simulations of boxes of side  $L = 5$  (top part of the table) and  $8\sigma$  (bottom part of the table) respectively.

| $\delta$ | $T_c^*$ | $\rho_c$ | $\mu_c$ |
|----------|---------|----------|---------|
| 0.005    | 0.2007  | 0.542    | -0.4817 |
| 0.01     | 0.2328  | 0.540    | -0.5614 |
| 0.02     | 0.2769  | 0.538    | -0.6693 |
| 0.03     | 0.3106  | 0.530    | -0.7575 |
| 0.04     | 0.3398  | 0.522    | -0.8333 |
| 0.05     | 0.3660  | 0.516    | -0.9042 |
| 0.10     | 0.4780  | 0.478    | -1.2120 |
| 0.05     | 0.3658  | 0.513    | -0.9062 |
| 0.10     | 0.4780  | 0.478    | -1.2138 |
| 0.20     | 0.667   | 0.421    | -1.7812 |
| 0.30     | 0.847   | 0.376    | -2.3505 |
| 0.40     | 1.029   | 0.339    | -2.9525 |
| 0.50     | 1.220   | 0.310    | -3.6002 |
| 0.60     | 1.430   | 0.287    | -4.3051 |
| 0.70     | 1.665   | 0.272    | -5.0890 |
| 0.80     | 1.940   | 0.263    | -5.9636 |

where the error bars are based on the spread of results from the different box sizes in this study.

Three important observations are in order:

i) Even for short-range interactions,  $B_2^{*c}$  shows a slight linear dependence on  $\delta$ , apparently contradicting the law of corresponding states. While this is technically correct, one must also remember that the small changes of  $B_2^{*c}$  with  $\delta$ , in the range  $0 < \delta < 0.05$  are not sufficient to produce any significant observable effect in the critical temperature estimated using a constant  $B_2^{*c}$  assumption via Eq. 2. This is due to the highly non-linear relationship between the two quantities, explaining the success of the law of corresponding states in the interpretation of simulation and experimental data of short-ranged attractive potentials.

From a more academic point of view, the law of corresponding states may still hold but with a scaling variable more complicated than the reduced virial coefficient itself and with a proper scaling of the density.

ii) The “best” critical parameters of the  $\delta = 0$  case are found to be different from those reported by Miller and Frenkel [20]. We believe this discrepancy is related to an incomplete mapping of the configuration space which manifests itself in a less complete sampling of the dense region. The extreme rarity of any hint of crystallization in the simulations of Miller and Frenkel is consistent with this proposed explanation.

iii) The higher critical temperature and density established by the SW extrapolation suggest that the Percus-Yevick energy route offers a more accurate estimate of the AHS critical point than the Percus-Yevick compressibility route.

We acknowledge support from MCRTN-CT-2003-504712 and J. L. MERG-CT-2006-046453. We thank D. Frenkel and G. Foffi for helpful discussions.

- 
- [1] M. H. J. Hagen, E. J. Meijer, G. C. A. M. Moolj, D. Frenkel, and H. N. W. Lekkerkerker, *Nature* **365**, 425 (1993).
  - [2] G. Pellicane, D. Costa, and C. Caccamo, *J. of Phys.: Condens. Matter* **16**, 4923 (2004), arXiv:cond-mat/0407335.
  - [3] D. Rosenbaum, P. C. Zamora, and C. F. Zukoski, *Phys. Rev. Lett.* **76**, 150 (1996).
  - [4] A. Lomakin, N. Asherie, and G. B. Benedek, *J. Chem. Phys.* **104**, 1646 (1996).
  - [5] W. C. K. Poon, *Phys. Rev. E* **55**, 3762 (1997).
  - [6] C. N. Likos, *Physics Reports* **348**, 267 (2001).
  - [7] M. G. Noro and D. Frenkel, *J. Chem. Phys.* **113**, 2941 (2000), arXiv:cond-mat/0004033.
  - [8] G. Foffi, C. D. Michele, F. Sciortino, and P. Tartaglia, *Phys. Rev. Lett.* **94**, 078301 (2005), arXiv:cond-mat/0410358.
  - [9] G. A. Vliegthart and H. N. W. Lekkerkerker, *J. Chem. Phys.* **112**, 5364 (2000).
  - [10] J. A. Barker and D. Henderson, *J. Chem. Phys.* **47**, 4714 (1967).
  - [11] R. J. Baxter, *J. Chem. Phys.* **49**, 2770 (1968).
  - [12] G. Stell, *J. Stat. Phys.* **63**, 1203 (1991).
  - [13] R. O. Watts, D. Henderson, and B. R. J., *Adv. Chem. Phys.* **21**, 421 (1971).

- [14] S. H. Chen, J. Rouch, F. Sciortino, and P. Tartaglia, *J. Phys.: Condens. Matter* **6**, 10855 (1994).
- [15] H. Verduin and J. K. G. Dhont, *J. Coll. Int. Sci.* **172**, 425 (1995).
- [16] C. Caccamo, *Physics Reports* **274**, 1 (1996).
- [17] N. A. Seaton and E. D. Glandt, *J. Chem. Phys.* **87**, 1785 (1987).
- [18] W. G. T. Kranendonk and D. Frenkel, *Mol. Phys.* **64**, 403 (1988).
- [19] S. B. Lee, *J. Chem. Phys.* **114**, 2304 (2001).
- [20] M. A. Miller and D. Frenkel, *Phys. Rev. Lett.* **90**, 135702 (2003), arXiv:cond-mat/0301550.
- [21] L. Vega, E. de Miguel, L. F. Rull, G. Jackson, and I. A. McLure, *J. Chem. Phys.* **96**, 2296 (1992).
- [22] F. Del Rio, E. Avalos, R. Espindola, L. F. Rull, G. Jackson, and S. Lago, *Mol. Phys.* **100**, 2531 (2002).
- [23] R. López-Rendón, Y. Reyes, and P. Orea, *J. Chem. Phys.* **125**, 4508 (2006).
- [24] D. L. Pagan and J. D. Gunton, *J. Chem. Phys.* **122**, 4515 (2005), arXiv:cond-mat/0412177.
- [25] H. Liu, S. Garde, and S. Kumar, *J. Chem. Phys.* **123**, 4505 (2005).
- [26] J. R. Elliott and L. Hu, *J. Chem. Phys.* **110**, 3043 (1999).
- [27] J. Chang and S. I. Sandler, *Mol. Phys.* **81**, 745 (1994).
- [28] A. D. Bruce and N. B. Wilding, *Phys. Rev. Lett.* **68**, 193 (1992).
- [29] N. B. Wilding, *J. Phys.: Condens. Matter* **9**, 585 (1997), arXiv:cond-mat/9610133.
- [30] G. Foffi and F. Sciortino, *J. Phys. Chem. B* **111**, 9702-9705 (2007).  
*J. Phys. Chem. B* 111, 9702-9705 (2007)
- [31] G. Foffi and F. Sciortino, *Phys. Rev. E* **74**, 050401 (2006), arXiv:cond-mat/0610885.
- [32] N. B. Wilding, *Phys. Rev. E* **52**, 602 (1995), arXiv:cond-mat/9503145.
- [33] M. A. Miller and D. Frenkel, *J. Phys.: Condens. Matter* **16**, 4901 (2004), arXiv:cond-mat/0406603.